Jurnal Ilmu Fisika
Vol. 16, No. 2, September 2024, pp. 142–150
ISSN: 1979-4657 (Print); 2614-7386 (Online)
https://doi.org/10.25077/jif.16.2.142-150.2024

Jurnal Ilmu Fisika
Open Access

Effect of Isopropanol on Optical Properties of Fe_3O_4/ZnO/Graphene Quantum Dots (GQDs) Nanocomposite

Sintha Widiawati, Astuti Astuti

Material Physics Laboratory, Department of Physics, Faculty of Mathematics and Natural Sciences, Universitas Andalas, Padang, 25163, Indonesia.

Article Info

Article History:

Received March 27, 2024
Revised June 23, 2024
Accepted July 21, 2024
Published online August 5, 2024

Keywords:

Fe_3O_4/ZnO
GQDs
nanocomposite
isopropanol

Corresponding Author:

Astuti Astuti,
Email: astuti@sci.unand.ac.id

ABSTRACT

This study aims to investigate the impact of isopropanol on the optical properties of the Fe_3O_4/ZnO/GQDs nanocomposite. The synthesis of Fe_3O_4 and ZnO nanoparticles was conducted using the coprecipitation method, followed by the synthesis of GQDs using the hydrothermal method with varying concentrations of isopropanol. Subsequently, the Fe_3O_4/ZnO nanocomposite was combined with GQDs synthesized using the sonication method. The amalgamation of magnetic and luminescent materials holds promise for applications in the biomedical field, particularly in bioimaging. XRD data analysis revealed crystal structure alterations attributed to the incorporation of carbon elements in both ZnO and Fe_3O_4. The TEM results indicated a particle size of 16.2 nm for the Fe_3O_4/ZnO/GQDs nanocomposite with a 10 ml isopropanol variation. Identified phases from the XRD analysis include Fe_3O_4, ZnO, and GQDs. UV-Vis spectroscopy detected distinctive absorbance peaks at wavelengths of 323.7 nm, 333.0 nm, 329.9 nm, and 323.9 nm. Moreover, the energy gap exhibited an increase with escalating concentrations of isopropanol in the GQDs. Photoluminescence analysis yielded robust, broad emission bands characterized by orange and red luminescence.

Copyright © 2024 Author(s)

1. INTRODUCTION

Nanoparticles are very small particles less than 100 nm in size and are widely developed, especially in the biomedical field. In this context, nanoparticles can be used for drug delivery (Rizvi & Saleh, 2018), magnetic resonance imaging (MRI) (Patsula et al., 2016), and bioimaging (Khosravanian et al., 2021). Bioimaging materials in the medical field typically use certain compounds to enhance visual contrast, such as Fe_3O_4 magnetic material, due to its superparamagnetic properties, biocompatibility, and ease of synthesis (Wu et al., 2015). Fe_3O_4 nanoparticles are a combination of iron oxide (Fe_2O_3) and iron monoxide (FeO).

The application of Fe_3O_4 as a contrasting material can be enhanced by combining it with a luminescent material. ZnO is one such luminescent material that is stable, biocompatible, and non-toxic (Reaz et al., 2020). Gupta et al. (2021) synthesized and characterized Fe_3O_4/ZnO nanocomposites, which exhibited superparamagnetic properties and strong emission, making these magnetic-luminescent materials promising for bioimaging applications. However, incorporating Fe_3O_4/ZnO nanocomposites

Attribution-NonCommercial 4.0 International

can decrease luminescence intensity, necessitating modification with luminescent materials such as graphene quantum dots (GQDs).

In recent years, carbon allotropes like diamond, carbon nanotubes, and graphene have garnered significant attention for supercapacitor applications (Gholinejad et al., 2017). GQDs offer several advantages, including low toxicity, small size, excellent photostability, biocompatibility, tunable photoluminescence properties, and ease of functionalization with biomolecules (Henna & Pramod, 2020). Additionally, they can be derived from abundant organic materials (Wang et al., 2016). Research by Wanas et al. (2023) successfully synthesized graphene/ZnO nanocomposites using ethanol solvents and the sonication method. The graphene/ZnO nanocomposite exhibited a wurtzite crystal structure, with photoluminescence (PL) characterization showing high and low emission peaks at 485 nm and 538 nm, corresponding to blue and green luminescence. SEM results indicated that the presence of ZnO on graphene prevents aggregation.

The GQDs synthesis process requires a solvent to dissolve certain compounds and form a homogeneous solution. Various solvents can be used, such as acetic acid, acetone, ethanol, nitric acid, hydrazine hydroxide (N_2H_5OH), and isopropanol. Isopropanol was chosen as the solvent in the GQDs manufacturing process due to its good solubility for various compounds (Fajarullah et al., 2014). Isopropanol is colorless, non-explosive, has a very strong odor, and dissolves easily in water (Goldsborough et al., 2021).

In this study, Fe_3O_4/ZnO/GQDs nanocomposite was synthesized using the sonication method, with rice husk serving as the carbon source for GQDs. The objective of this study is to analyze the effect of isopropanol on the optical properties of Fe_3O_4/ZnO/GQDs nanocomposite with isopropanol variations of 5 ml, 7.5 ml, and 10 ml, aiming to enhance the utility of these magnetic-luminescent materials for bioimaging applications.

2. METHOD

2.1 Synthesis of Fe_3O_4/ZnO Nanocomposite

Fe_3O_4/ZnO/GQDs nanocomposite were synthesized using the following materials: Iron (III) chloride hexahydrate ($FeCl_3 \cdot 6H_2O$, Merck), iron (II) sulfate heptahydrate ($FeSO_4 \cdot 7H_2O$, Merck), ammonium hydroxide (NH_4OH 21%, Bratachem), alcohol 96%, zinc nitrate ($Zn(NO_3)_2$, Merck), polyethylene glycol (Merck), and isopropanol (Bratachem). Fe_3O_4 nanoparticles were synthesized using the coprecipitation method. This method involved dissolving $FeCl_3 \cdot 6H_2O$ and $FeSO_4 \cdot 7H_2O$ with a molarity ratio of 2:1 in 30 ml of distilled water. Once the solution was homogeneous, 30 ml of NH_4OH was gradually added until the solution turned solid black. The solution was stirred with a magnetic stirrer at 60℃ for 180 minutes. The resulting solid was precipitated using a permanent magnet and washed with distilled water three times.

In the next step, zinc nitrate was dissolved in 100 ml of distilled water, and 30 ml of NH_4OH was gradually added. This zinc nitrate solution was mixed into the Fe_3O_4 precipitate and stirred using a magnetic stirrer at 70℃ for 24 hours. The mixture was then precipitated with a permanent magnet and washed with distilled water three times. The obtained precipitate was dried in a furnace at 300℃ for 2 hours. The dried precipitate was then crushed to form Fe_3O_4/ZnO nanocomposite powder.

2.2 Synthesis of Graphene Quantum Dots (GQDs)

The synthesis of GQDs from rice husk was carried out using the hydrothermal method. Initially, the rice husk was cleaned to remove dust and soil impurities. The cleaned rice husk was then dried in an oven at 110℃ for 2 hours to reduce water content. Subsequently, it was placed in a furnace at 400℃ for 2 hours until it became carbon (charcoal). Next, 0.2 grams of rice husk carbon powder was mixed with 5 ml, 7.5 ml, and 10 ml of isopropanol, and dissolved in 50 ml of distilled water. This mixture was then sonicated for 30 minutes to improve the homogeneity of the solution. After sonication, the solution was transferred to an autoclave and heated at 200℃ for 6 hours. Following this, the solution underwent

a filtration process using 0.2 mm Wattman filter paper to separate the carbon deposits, which were then dried. The resulting precipitate was placed in a furnace at 200℃ for 10 hours. Finally, the dried precipitate was crushed to produce GQDs powder.

2.3 Synthesis of Fe_3O_4/ZnO/GQDs Nanocomposite

The synthesis of Fe_3O_4/ZnO/GQDs nanocomposite was carried out using the sonication method. A total of 0.2 grams of Fe_3O_4/ZnO nanocomposite and 0.05 grams of GQDs were weighed and then dissolved in 30 ml of distilled water. Once dissolved, the solution was sonicated for 1 hour. The sonicated solution was then centrifuged to separate the precipitate. The resulting precipitate was placed in a furnace at 200℃ for 1 hour. The dried precipitate was then crushed to produce Fe_3O_4/ZnO/GQDs nanocomposite powder.

The flow chart in Figure 1 illustrates the research process for the Fe_3O_4/ZnO/GQDs nanocomposite.

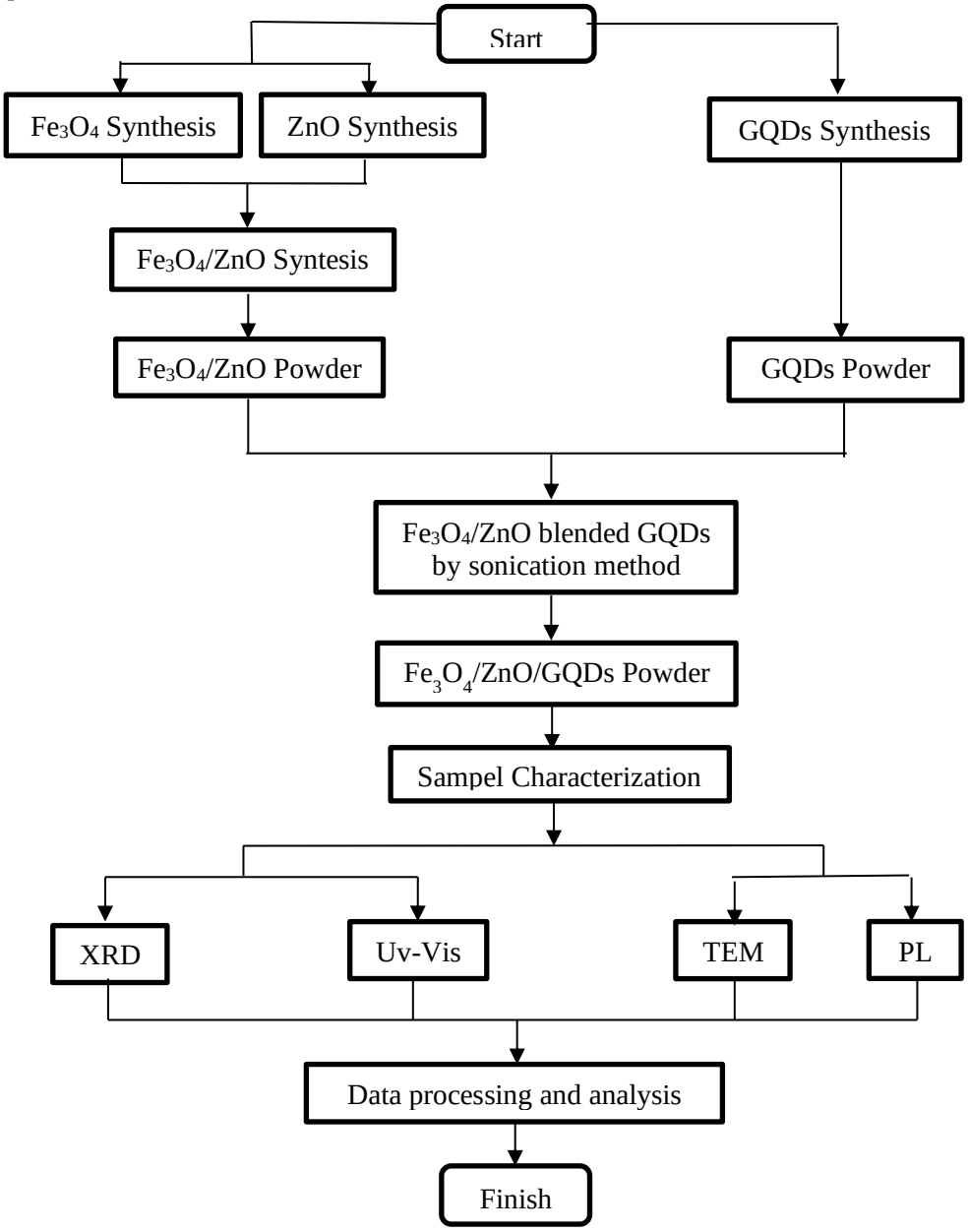

Figure 1 Research flow chart.

2.4 Characterization

The synthesized nanocomposite was characterized using an X-ray diffractometer (Bruker D8 Advance), a UV-Vis spectrophotometer, photoluminescence (Horiba MicrO Photoluminescence Microspectrometer), and transmission electron microscopy (FEI Tecnai G2 20 S-Twin). The determination of crystal size in Fe_3O_4/ZnO/GQDs nanocomposite samples was calculated based on the Debye-Scherrer Equation, systematically presented in Equation (1).

$$D = \frac{K\lambda}{B\cos\theta} \tag{1}$$

where D is the nanoparticle crystalline size (nm) , K is crystal dimension (0.9), λ is wavelength of the X-ray used (nm), B is half-maximum peak width (rad) and θ is X-ray diffraction angle.

3. RESULTS AND DISCUSSION

3.1 Structure and Size Analysis

XRD characterization aims to determine the structure and crystal size of the Fe_3O_4/ZnO/GQDs nanocomposite with varying concentrations of isopropanol. Figure 2 presents the X-ray diffraction pattern of Fe_3O_4/ZnO nanocomposites and Fe_3O_4/ZnO/GQDs nanocomposites with different isopropanol variations.

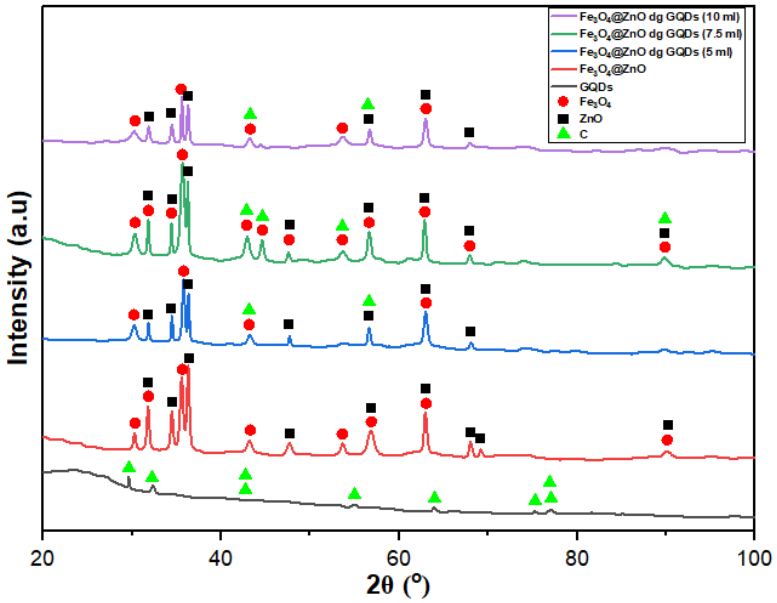

Figure 2 X-ray diffraction patterns of Fe_3O_4/ZnO nanocomposites and Fe_3O_4/ZnO/GQDs nanocomposites with isopropanol variation.

The diffraction pattern of the Fe_3O_4/ZnO/GQDs nanocomposite with 5 ml of isopropanol shows the highest diffraction peak at an angle 2θ = 35.7322°. According to the International Diffraction Database (ICDD) standard data, the crystal structures formed are Fe_3O_4 (cubic), ZnO (hexagonal), and carbon (rhombohedral). The Fe_3O_4/ZnO/GQDs nanocomposite with 7.5 ml of isopropanol exhibits the highest diffraction peak at 2θ = 35.6193°. Based on ICDD standard data, the crystal structures formed are Fe_3O_4 (orthorhombic), ZnO (hexagonal), and carbon (hexagonal). The Fe_3O_4/ZnO/GQDs nanocomposite with 10 ml of isopropanol shows the highest diffraction peak at 2θ = 35.5531°. According to ICDD standard data, the crystal structures formed are Fe_3O_4 (cubic), ZnO (hexagonal), and carbon (hexagonal).

The maximum diffraction peak produced by the Fe_3O_4/ZnO/GQDs nanocomposite decreases due to the presence of carbon in the Fe_3O_4/ZnO nanocomposite, which affects the crystal structure. This results in a broadening of the diffraction peak and a decrease in intensity (Manikandan et al., 2020). The differing crystal structures of the Fe_3O_4/ZnO/GQDs nanocomposites with varying isopropanol concentrations are attributed to changes in the crystal structure due to the addition of carbon elements in ZnO and Fe_3O_4. When Fe_3O_4 or carbon is mixed with other compounds, it forms new compounds, such as Fe_3O_4/ZnO nanocomposites and Fe_3O_4/ZnO/GQDs nanocomposites (Selezneva et al., 2022). The crystal structure of ZnO is hexagonal wurtzite, the most stable form (Morkoç & Özgür, 2008). The crystal structure of Fe_3O_4 is cubic (Gupta et al., 2021). The crystal size of the Fe_3O_4/ZnO/GQDs nanocomposite with three isopropanol variations, as determined using the Scherrer Equation, is presented in Table 1.

Table 1 Crystal size.

Sample		λ (nm)	B (rad)	Cos θ	D (nm)
Fe_3O_4/ZnO	Fe_3O_4	0.15	0.0071	0.46	42.03
	ZnO	0.15	0.0054	0.75	34.5
Fe_3O_4/ZnO/GQDs (5 ml)	Fe_3O_4	0.15	0.0054	0.55	46.72
	ZnO	0.15	0.0027	0.77	67.33
Fe_3O_4/ZnO/GQDs (7.5 ml)	Fe_3O_4	0.15	0.0089	0.5	30.68
	ZnO	0.15	0.0027	0.74	70.10
Fe_3O_4/ZnO/GQDs (10 ml)	Fe_3O_4	0.15	0.0027	0.48	108.44
	ZnO	0.15	0.0044	0.74	41.73

The largest crystal size is found in the Fe_3O_4/ZnO/GQDs nanocomposite (10 ml), measuring 108.4443 nm, while the smallest crystal size is in the Fe_3O_4/ZnO/GQDs nanocomposite (7.5 ml), measuring 30.67967 nm. The width of the diffraction peak is inversely related to the crystal size; smaller crystal sizes exhibit a larger Full Width at Half Maximum (FWHM), resulting in broader diffraction peaks (Lapailaka & Triandi, 2013). According to Gupta et al. (2021), smaller crystal sizes can affect the crystal structure, and a more ordered crystal structure can improve the optical properties of the material.

The particle size was characterized using High-Resolution Transmission Electron Microscopy (HR-TEM). The TEM test results are shown in Figure 3. The TEM results for the Fe_3O_4/ZnO/GQDs nanocomposite (10 ml) in Figure 3b highlight sections indicating the formation of reflections corresponding to the Fe_3O_4, ZnO, and GQDs phases. From the high-resolution HR-TEM image (Figure 3b), the lattice pattern of Fe_3O_4 is not visible, likely due to the thick ZnO layer. However, the dark-colored particles observed in the HR-TEM images are attributed to Fe_3O_4 nanoparticles, while the bright particles are attributed to ZnO nanoparticles (Gupta et al., 2021). GQDs are derived from particles with a crystal structure consisting of thin graphene layers in hexagonal patterns (Ganganboina et al., 2017).

The average particle size of the Fe_3O_4/ZnO/GQDs nanocomposite (10 ml) is 16.2 nm. Comparing the XRD results for crystal size with the TEM results for average particle size reveals a discrepancy. This difference may be due to aggregation, agglomeration (Ramanenka et al., 2020), or even crystal defects in the Fe_3O_4/ZnO/GQDs nanocomposite. These factors can affect the width of the diffraction peaks in the XRD results and complicate the identification of individual particles, making them appear smaller (Gupta et al., 2021).

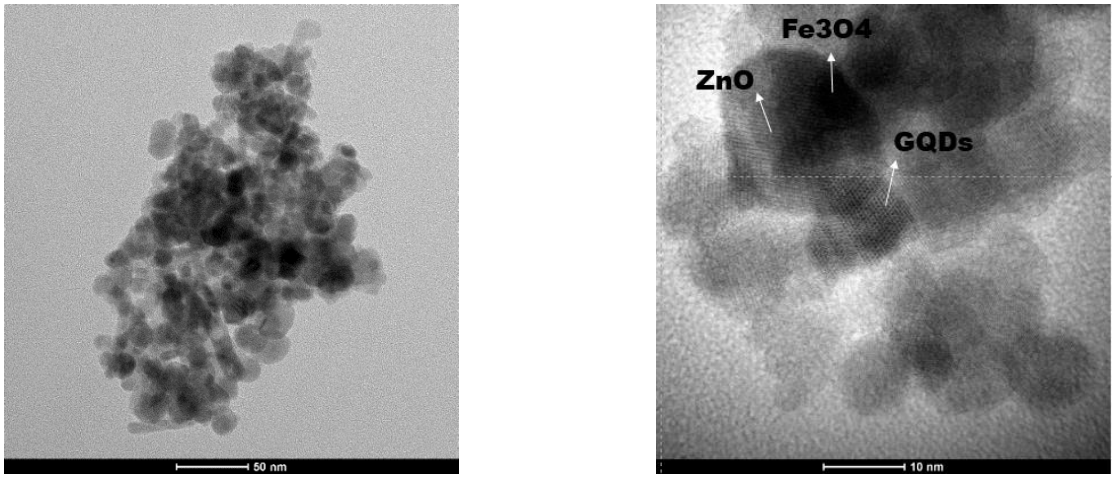

(a) (b)

Figure 3 (a) TEM results of Fe_3O_4/ZnO/GQDs nanocomposite (10 ml) with a scale of 50 nm and (b) TEM results of Fe_3O_4/ZnO/GQDs nanocomposite (10 ml) with a scale of 10 nm.

3.2 UV-Vis Spectrophotometer Analysis

UV-Vis spectrophotometer characterization was used to determine the absorbance spectrum and energy band gap width. The absorbance spectra of Fe_3O_4/ZnO/GQDs nanocomposites with three variations of isopropanol concentration are shown in Figure 4.

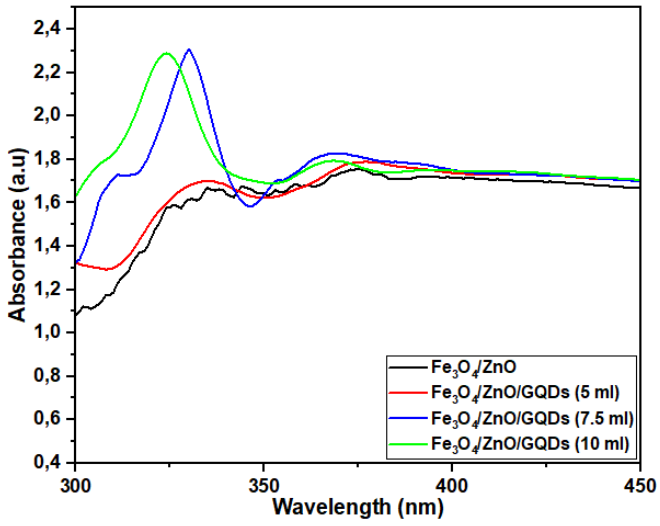

Figure 4 Absorbance spectra of Fe_3O_4/ZnO nanocomposite and Fe_3O_4/ZnO /GQDs nanocomposite with isopropanol variation.

The absorbance spectrum analysis shows that the wavelengths of Fe_3O_4/ZnO nanocomposite and Fe_3O_4/ZnO/GQDs nanocomposite with varying isopropanol concentrations can absorb light within the 300-400 nm range, which is within the visible light spectrum. In the Fe_3O_4/ZnO nanocomposite, light absorption occurs below 400 nm, concentrating some light in the UV region (Xu et al., 2023). However, the presence of GQDs in the Fe_3O_4/ZnO nanocomposite results in continuous absorbance in the visible light region as the isopropanol concentration in the GQDs increases (Liang et al., 2020).

The energy band gap value was determined based on the absorbance spectrum, which was then processed using the Tauc plot method. The results of the energy band gap values for Fe_3O_4/ZnO

nanocomposite and Fe_3O_4/ZnO/GQDs nanocomposite with varying isopropanol concentrations are shown in Figure 5.

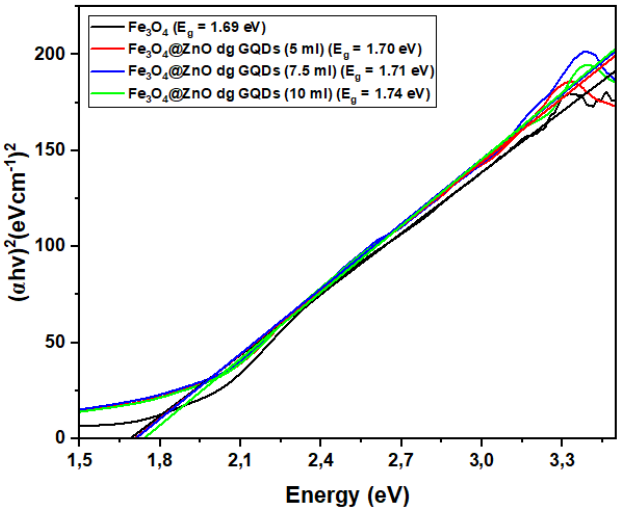

Figure 5 Energy band gap values of Fe_3O_4/ZnO nanocomposite and Fe_3O_4/ZnO /GQDs nanocomposite with isopropanol variation

The energy band gap value obtained is different for each sample. For the Fe_3O_4/ZnO nanocomposite, the band gap is 1.69 eV. For the Fe_3O_4/ZnO/GQDs nanocomposite with 5 ml of isopropanol, the band gap is 1.70 eV; with 7.5 ml of isopropanol, the band gap is 1.71 eV; and with 10 ml of isopropanol, the band gap is 1.74 eV. Based on these results, the energy band gap value increases with the addition of isopropanol to the GQDs. The GQDs, which possess good mechanical properties and high electrical conductivity, can be effectively influenced by the presence of the Fe_3O_4/ZnO nanocomposite (Jana & Scheer, 2018).

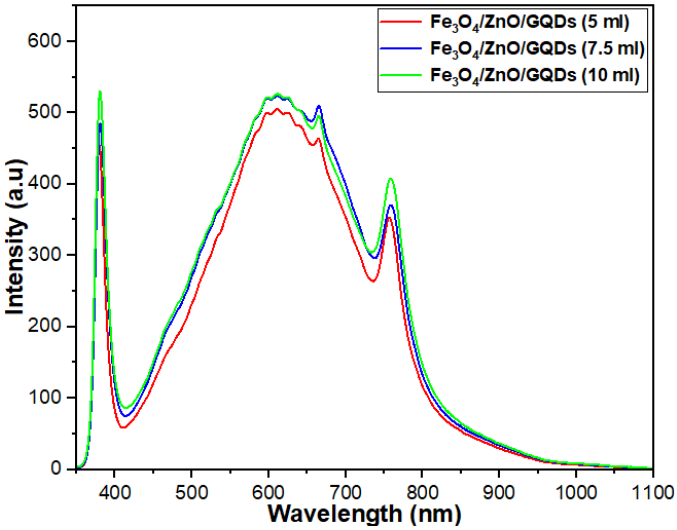

Figure 6 Photoluminescence result of Fe_3O_4/ZnO nanocomposite and Fe_3O_4/ZnO/GQDs nanocomposite with isopropanol variation.

3.3 Photoluminescence (PL) Spectroscopy Analysis

PL characterization was performed to determine the luminous properties of Fe_3O_4/ZnO/GQDs nanocomposite with varying isopropanol concentrations. PL characterization uses laser light at 325 nm

to produce the spectrum shown in Figure 6. The photoluminescence results of Fe_3O_4/ZnO/GQDs nanocomposites with isopropanol variations show the same wavelength range (350-1100 nm) and the same emission peaks, producing two strong and sharp emission bands centered around 380 nm (UV emission peak) and different intensity values. The near-band edge (NBE) the UV emission peak indicates excitons from the optical activity of ZnO's intrinsic defects. The visible light emission peak (λ = 500–780 nm) in the second band is indicative of deep-level defects (DLE) in ZnO. The PL spectrum can be well dispersed after mixing with varying concentrations of isopropanol in GQDs; the role of isopropanol can improve optical properties and increase luminescence (Ramanenka et al., 2020). The interaction between Fe_3O_4/ZnO and GQDs in the Fe_3O_4/ZnO/GQDs nanocomposite increases luminescence (Sajjad et al., 2018) due to changes in light emission in Fe_3O_4/ZnO after mixing GQDs with isopropanol variations (Deng et al., 2017).

The broad emission peak contains five characteristic peaks: orange emission bands centered at 597 nm and 611 nm, and red emission bands centered at 626 nm, 641 nm, and 665 nm. The second relatively strong emission peak is centered at 759 nm. The luminescence in each sample when GQDs are applied to Fe_3O_4/ZnO nanocomposites is influenced by factors from the solvent and doping effects (Zhu et al., 2015). The appearance of strong and broad emission peaks indicates that Fe_3O_4/ZnO/GQDs nanocomposites are suitable for bioimaging applications (Gupta et al., 2021).

4. CONCLUSION

The crystal structure of the Fe_3O_4/ZnO/GQDs nanocomposite varies with isopropanol concentration due to changes in the crystal structure from adding carbon elements into ZnO and Fe_3O_4. The largest crystal size is found in the Fe_3O_4/ZnO/GQDs nanocomposite with 10 ml of isopropanol, with an average particle size of 16.2 nm. The smallest crystal size is found in the Fe_3O_4/ZnO/GQDs nanocomposite with 7.5 ml of isopropanol. UV-Vis results show that Fe_3O_4/ZnO nanocomposite and variations of Fe_3O_4/ZnO/GQDs nanocomposite have different absorbance peaks at wavelengths of 323.7 nm, 333.0 nm, 329.9 nm, and 323.9 nm. The band gap values obtained are 1.69 eV, 1.70 eV, 1.71 eV, and 1.74 eV, respectively. PL results show a wavelength range of 350-1100 nm, producing a strong, sharp emission peak centered at 380 nm. The resulting photoluminescence colors are orange and red.

ACKNOWLEDGEMENT

The author would like to thank the Directorate of Learning and Student Affairs, Directorate General of Higher Education, Research and Technology for funding this research through PKM 2023 activities.

REFERENCE

Deng, J., Lu, D., Zhang, X., Shi, G., & Zhou, T. (2017). Highly sensitive GQDs-MnO2 based assay with turn-on fluorescence for monitoring cerebrospinal acetylcholinesterase fluctuation: A biomarker for organophosphorus pesticides poisoning and management. *Environmental Pollution*, *224*, 436–444.

Fajarullah, A., Irawan, H., & Pratomo, A. (2014). Ekstraksi Senyawa Metabolit Sekunder Lamun Thalassodendron Ciliatum Pada Pelarut Berbeda. *Repository Umrah*, *1*(1), 1–15.

Ganganboina, A. B., Chowdhury, A. D., & Doong, R. (2017). Nano assembly of N-doped graphene quantum dots anchored Fe3O4/halloysite nanotubes for high performance supercapacitor. *Electrochimica Acta*, *245*, 912–923.

Gholinejad, M., Ahmadi, J., Najera, C., Seyedhamzeh, M., Zareh, F., & Kompany-Zareh, M. (2017). Graphene quantum dot modified Fe3O4 nanoparticles stabilize PdCu nanoparticles for enhanced catalytic activity in the Sonogashira reaction. *ChemCatChem*, *9*(8), 1442–1449.

Goldsborough, S. S., Cheng, S., Kang, D., Saggese, C., Wagnon, S. W., & Pitz, W. J. (2021). Effects of isoalcohol blending with gasoline on autoignition behavior in a rapid compression machine: isopropanol and isobutanol. *Proceedings of the Combustion Institute*, *38*(4), 5655–5664.

Gupta, J., Hassan, P. A., & Barick, K. C. (2021). Core-shell Fe3O4@ ZnO nanoparticles for magnetic hyperthermia and bio-imaging applications. *AIP advances*, *11*(2).

Henna, T. K., & Pramod, K. (2020). Graphene quantum dots redefine nanobiomedicine. *Materials Science and Engineering: C*, *110*, 110651.

Jana, A., & Scheer, E. (2018). Study of optical and magnetic properties of graphene-wrapped ZnO nanoparticle hybrids. *Langmuir*, *34*(4), 1497–1505.

Khosravanian, A., Moslehipour, A., & Ashrafian, H. (2021). A review on bioimaging, biosensing, and drug delivery systems based on graphene quantum dots. *Prog. Chem. Biochem. Res*, *4*, 44.

Lapailaka, T., & Triandi, R. (2013). Penentuan ukuran Kristal (crystallite size) lapisan tipis PZT dengan metode XRD melalui pendekatan persamaan Debye Scherrer. *Erudio Journal of Educational Innovation*, *1*(2).

Liang, H., Tai, X., Du, Z., & Yin, Y. (2020). Enhanced photocatalytic activity of ZnO sensitized by carbon quantum dots and application in phenol wastewater. *Optical Materials*, *100*, 109674.

Manikandan, A., Yogasundari, M., Thanrasu, K., Dinesh, A., Raja, K. K., Slimani, Y., Jaganathan, S. K., Srinivasan, R., & Baykal, A. (2020). Structural, morphological and optical properties of multifunctional magnetic-luminescent ZnO@ Fe3O4 nanocomposite. *Physica E: Low-dimensional Systems and Nanostructures*, *124*, 114291.

Morkoç, H., & Özgür, Ü. (2008). *Zinc oxide: fundamentals, materials and device technology*. John Wiley & Sons.

Patsula, V., Kosinová, L., Lovrić, M., Ferhatovic Hamzić, L., Rabyk, M., Konefal, R., Paruzel, A., Šlouf, M., Herynek, V., & Gajović, S. (2016). Superparamagnetic Fe3O4 nanoparticles: synthesis by thermal decomposition of iron (III) glucuronate and application in magnetic resonance imaging. *ACS applied materials & interfaces*, *8*(11), 7238–7247.

Ramanenka, A. A., Lizunova, A. A., Mazharenko, A. K., Kerechanina, M. F., Ivanov, V. V, & Gaponenko, S. V. (2020). Preparation and Optical Properties of Isopropanol Suspensions of Aluminum Nanoparticles. *Journal of Applied Spectroscopy*, *87*(4).

Reaz, M., Haque, A., Cornelison, D. M., Wanekaya, A., Delong, R., & Ghosh, K. (2020). Magneto-luminescent zinc/iron oxide core-shell nanoparticles with tunable magnetic properties. *Physica E: Low-dimensional Systems and Nanostructures*, *123*, 114090.

Rizvi, S. A. A., & Saleh, A. M. (2018). Applications of nanoparticle systems in drug delivery technology. *Saudi pharmaceutical journal*, *26*(1), 64–70.

Sajjad, M., Makarov, V., Sultan, M. S., Jadwisienczak, W. M., Weiner, B. R., & Morell, G. (2018). Synthesis, optical, and magnetic properties of graphene quantum dots and iron oxide nanocomposites. *Advances in Materials Science and Engineering*, *2018*(1), 3254081.

Selezneva, N. V, Nosovets, V. S., Sherokalova, E. M., Shishkin, D. A., & Baranov, N. V. (2022). Crystal structure and properties of layered compounds Fe0. 75TiS2–ySey. *Solid State Sciences*, *134*, 107049.

Wanas, W., Abd El-Kaream, S. A., Ebrahim, S., Soliman, M., & Karim, M. (2023). Cancer bioimaging using dual mode luminescence of graphene/FA-ZnO nanocomposite based on novel green technique. *Scientific Reports*, *13*(1), 27.

Wang, L., Li, W., Wu, B., Li, Z., Wang, S., Liu, Y., Pan, D., & Wu, M. (2016). Facile synthesis of fluorescent graphene quantum dots from coffee grounds for bioimaging and sensing. *Chemical Engineering Journal*, *300*, 75–82.

Wu, M., Zhang, D., Zeng, Y., Wu, L., Liu, X., & Liu, J. (2015). Nanocluster of superparamagnetic iron oxide nanoparticles coated with poly (dopamine) for magnetic field-targeting, highly sensitive MRI and photothermal cancer therapy. *Nanotechnology*, *26*(11), 115102.

Xu, J.-J., Lu, Y.-N., Tao, F.-F., Liang, P.-F., & Zhang, P.-A. (2023). ZnO nanoparticles modified by carbon quantum dots for the photocatalytic removal of synthetic pigment pollutants. *ACS omega*, *8*(8), 7845–7857.

Zhu, C., Yang, S., Wang, G., Mo, R., He, P., Sun, J., Di, Z., Yuan, N., Ding, J., & Ding, G. (2015). Negative induction effect of graphite N on graphene quantum dots: tunable band gap photoluminescence. *Journal of Materials Chemistry C*, *3*(34), 8810–8816.